

A Dynamical Study of the Disordered Quantum $p = 2$ Spherical Model

Michal Rokni and Premala Chandra

Chandra Tech Consulting LLC, 123 Harper Street, Highland Park, NJ 08904

Abstract

We present a dynamical study of the disordered quantum $p = 2$ spherical model at long times. Its phase behavior as a function of spin-bath coupling, strength of quantum fluctuations and temperature is characterized, and we identify different paramagnetic and coarsened regions. A quantum critical point at zero temperature in the limit of vanishing dissipation is also found. Furthermore we show analytically that the fluctuation-dissipation theorem is obeyed in the stationary regime, an assumption that is made routinely for more complex glassy models.

I. INTRODUCTION

The dynamics of quantum systems far from equilibrium present many conceptual challenges, particularly in the area of quantum glasses. The classical analogues of these systems display broad relaxation spectra; furthermore their long-time behavior depends explicitly on details of sample history. In this paper a motivating question is whether the introduction of quantum fluctuations in a classical system out of equilibrium results in qualitatively new behavior at long time-scales. To date, the introduction of quantum fluctuations in theoretical glassy models has not led to qualitative changes, e.g., new slow quantum modes, in their long-time dynamics [1–5]. In hindsight one can understand these results by noting that all these systems have finite decoherence times beyond which they age classically, in part due to the fact that they all include finite dissipation. From another perspective, quantum fluctuations often drive the glass transition to be first-order [6–10], and thus only qualitatively affect the dynamical behavior on *short*-time scales. The only known exceptions occur when, in the absence of dissipation, quantum fluctuations do not lead to a first-order transition at zero temperature, but rather to a quantum critical point. This occurs in two mean-field models: that of the periodic Josephson array [11], and that of the infinite-component quantum rotors [12, 13]. Detailed characterization of the phase space as a function of dissipation, temperature, and quantum fluctuations remains to be studied in both cases.

Careful experimental studies of the dipolar magnet $\text{LiHo}_x\text{Y}_{1-x}\text{F}_4$ indicate that the current theoretical picture of quantum glassy systems is not the full story [14]. An appropriate model for the description of the magnetic properties of this material consists of Ising spins, representing the states of the magnetic ions, residing on random sites, and interacting via short-range ferromagnetic couplings and long-range dipole-dipole interactions. The sign of the latter interaction depends on the relative position of the spins, leading to the possibility of competing interactions and to frustration. For $x = 1$, the short-range component of the interaction dominates and the system is a ferromagnet. However, the Curie temperature decreases as x is reduced. The effects of quantum mechanics can be tuned in this system by application of a magnetic field transverse to the spins. Even in the disordered ferromagnetic state ($x \sim 0.4$), there are qualitative effects of the transverse field, particularly near the observed quantum critical point, that have not been described by theoretical models [14–16].

Motivated by these experiments, we study the dynamics of a long-range quantum disordered ferromagnet, the quantum spherical model with Gaussian random two-spin interactions ($p = 2$). Classically the statics of this model are trivial, as the free energy has only two minima, and it can be solved exactly with a replica symmetric ansatz [17]. However, for almost any initial conditions, the dynamics of this classical system are out-of equilibrium with power-law decays in many of the observed quantities [18]. The origin of this slow relaxation is very different from that of classical mean-field spin glasses. In these latter systems the time evolution is determined by the complex structure of the phase space [19]. By contrast the free energy landscape of the $p = 2$ case is very simple. However, statistically the overlap between the initial and the equilibrium configurations is very small. This is qualitatively similar to the situation in a weakly disordered ferromagnet after a rapid temperature quench where the resulting domain structure bears little resemblance to the uniform equilibrium state. For this reason we refer to the non-ergodic phases of the $p = 2$ spherical model as coarsened.

Naturally the infinite-range nature of this Hamiltonian implies the absence of any length-scale in real-space. The spherical character of the spins combined with the quadratic interaction lead to reduced nonlinearities in this disordered $p = 2$ model, even compared to other mean-field spin glasses. These two key features, specifically the infinite-range coupling and the minimal nonlinearities, make this model amenable to analytic treatment, and it can serve as a testing ground for necessary assumptions made in more complicated glassy systems. The disordered quantum $p = 2$ spherical model bears a strong resemblance to that of the infinite-range M -component quantum rotors in the limit $M \rightarrow \infty$ [12, 13]. More explicitly, the M -component quantum rotor Hamiltonian is composed of M replicas which each individually resemble the $p = 2$ system, where the inter-replica coupling scales inversely with M [13]. Here we extend previous studies of these and related rotor Hamiltonians [5, 12, 13] by performing a detailed characterization of the phase behavior of the disordered quantum $p = 2$ spherical model, noting that our results recover those previously obtained in particular well-defined limits.

In this paper we characterize the phase behavior of the disordered $p = 2$ spherical model as a function of quantum and thermal fluctuations and the spin-bath coupling, and identify its distinct paramagnetic and coarsened regions by studying its long-time dynamical behavior. Known results are reproduced in both the high- and the zero- temperature limits, where the

latter is in the absence of finite dissipation. We also demonstrate analytically the validity of an ansatz routinely employed in the study of more complex glasses [1–4], namely that the fluctuation-dissipation theorem remains valid in the stationary regime.

The plan of the paper is as follows. In Section II we present the model. Its dynamical equations, which we derive using the Keldysh formalism, are discussed in Section III. The stationary parts of the retarded and the statistical Green functions, that we find in Section IV, are then shown analytically to obey the fluctuation-dissipation theorem. In Section V an expression for the Edwards-Anderson order parameter is presented with the resulting emergence of a quantum critical point. Details of the phase diagram are discussed in Section VI for all the coarsened and the paramagnetic regions. We end with a discussion, Section VII, where after summarizing the main features of this work, we mention several open questions that emerge from our study.

II. FORMULATION OF THE PROBLEM

In this paper we study the dynamics of the disordered quantum $p = 2$ spherical spin glass model coupled to an Ohmic bath. There are N spins that can be written in vector form as $\mathbf{s} = (s_1, s_2, \dots, s_N)$, and we will assume that $N \rightarrow \infty$. The Hamiltonian of the system takes the form

$$\mathcal{H} = \mathcal{H}_0 + \mathcal{H}_{\text{SS}} + \mathcal{H}_{\text{B}} + \mathcal{H}_{\text{SB}}, \quad (1)$$

where \mathcal{H}_0 , \mathcal{H}_{SS} , \mathcal{H}_{B} and \mathcal{H}_{SB} are the free, the spin-spin, the bath, and the spin-bath contributions respectively.

In the absence of interactions the free Hamiltonian of the spin system is given by

$$\mathcal{H}_0 = \frac{\boldsymbol{\pi}^2}{2m}, \quad (2)$$

where the conjugated momenta $\boldsymbol{\pi} = (\pi_1, \pi_2, \dots, \pi_N)$ obey the usual commutation relations $[s_i, s_j] = [\pi_i, \pi_j] = 0$, and $[\pi_i, s_j] = -i\delta_{ij}$; here we use a unit system where $\hbar = k_B = 1$. The “mass” m is a constant that introduces dynamics into the problem. As we will explain below, the dynamics of the system can be tuned from the classical to the quantum regimes by varying the mass m . We note that there are other methods of quantization (e.g. application of a transverse field) besides this “kinetic” one; if done correctly, they should all yield the same results [6].

The spins interact with each other via a spin-spin interaction which, for the $p = 2$ model, is given by

$$\mathcal{H}_{\text{SS}}[J] = \sum_{i_1 < i_2}^N J_{i_1 i_2} s_{i_1} s_{i_2}, \quad (3)$$

with randomly distributed matrix elements J_{ij} , that obey $\overline{J_{ij}} = 0$, $\overline{J_{ij} J_{kl}} \Big|_{i \neq k \text{ or } j \neq l} = 0$, and $\overline{J_{ij}^2} = J^2/N$, where $\overline{\dots}$ represents averaging over the random spin-spin interaction.

In the spherical model the spins, s_i , are constrained to a spherical surface such that $\sum_{i=1}^N \overline{\langle s_i^2 \rangle} = N$, where $\langle \dots \rangle$ represent quantum averaging. Thus s_i are continuous variables, that behave like coordinates. However, since this model has been introduced as an analytically accessible spin problem, we will keep the notation and the nomenclature. The spherical constraint is initially introduced into the Lagrangian, which results in the additional term, $-\frac{1}{2} z(t) \mathbf{s}^2$, in the Hamiltonian. The time-dependent function, $z(t)$, is a Lagrange multiplier. Thus the free Hamiltonian \mathcal{H}_0 (2), is effectively replaced by

$$\mathcal{H}_0 = \frac{\pi^2}{2m} - \frac{1}{2} z(t) \mathbf{s}^2. \quad (4)$$

Each spin in the system is connected to a system of N_B independent harmonic oscillators that constitute the bath. The free Hamiltonian of the bath is given by

$$\mathcal{H}_B = \frac{1}{2} \sum_{a=1}^{N_B} \left[\frac{\mathbf{P}_a^2}{M_a} + M_a \omega_a^2 \mathbf{x}_a^2 \right], \quad (5)$$

where $\mathbf{x}_a = (x_{a1}, x_{a2}, \dots, x_{aN})$ are the oscillator coordinates of mode a , and x_{ai} is the coordinate of the oscillator that interacts with spin s_i . The conjugate momenta $\mathbf{P}_a = (P_{a1}, P_{a2}, \dots, P_{aN})$ are related to \mathbf{x}_a through the commutation relations $[x_{ai}, x_{aj}] = [P_{ai}, P_{aj}] = 0$, and $[P_{ai}, x_{aj}] = -i\delta_{ij}$. The mass and frequency of mode a of the oscillators are given by M_a and ω_a , respectively. For simplicity we assume a linear interaction between the spins and the bath [20]

$$\mathcal{H}_{\text{SB}}[C_a] = \sum_{a=1}^{N_B} C_a \mathbf{x}_a \cdot \mathbf{s}, \quad (6)$$

where the coupling coefficients are given by C_a . We are aware that this model for a bath can lead to unwanted divergencies due to low-frequency contributions in the absence of an infrared cut-off [21]. However, this problem does not arise in our case due to the structure of the relevant spectral density, as we discuss later in the paper. Such a simple interaction between the spin system and the bath allows us to solve the problem analytically. Since we

are interested in the spin system at long times we assume that the specific form of the bath is not important.

The Hamiltonian for the spin system is actually that of a harmonic oscillator. Because the coupling to the bath (6) is linear in the spin operator, it does not alter this statement. In the paramagnetic phase the spin-spin interaction is negligible, and we recognize that $\sqrt{z(t)/m}$ is the eigenenergy of the oscillator. We are interested in the long-time behavior of $z(t)$ when it saturates to a constant z_∞ . In order to understand whether the dynamics of the spin system are governed by classical or quantum fluctuations, we compare the important energy-scale of the system to the temperature T . At constant T when m is increased, the eigenenergy of the spin Hamiltonian decreases. Once the dominant energy-scale is smaller than T , the system dynamics are governed by classical behavior. Similarly, when m is decreased, T becomes smaller than the dominant energy-scale, and quantum dynamics become more important. As a cautionary aside, we note that z_∞ may depend on m in the paramagnetic regime; however we will show that to leading order it is either independent of m or proportional to m^{-1} , so that the preceding heuristic argument is still valid.

In the coarsened phase the spin-spin coupling cannot be neglected. After averaging over this interaction, it is harder to recognize the eigenenergies. However, the results presented here indicate that when the coupling to the bath is infinitesimal, the signatory parameter is $x = \sqrt{mT^2/J}$: for x large, the dynamics are dominated by classical effects whereas for x small quantum effects are involved. It is only at $T = 0$ that the dynamics are purely quantum in nature. We conclude therefore that the energy-scales T and $\sqrt{J/m}$ should be compared in order to find whether the dynamics are purely classical or partially quantum (except at $T = 0$). This is consistent with the previous discussion of the paramagnetic phase, where small mass corresponds to a regime where quantum fluctuations could become dominant.

III. THE DYSON EQUATIONS FOR THE SPIN GREEN FUNCTIONS

The dynamics of the spin system can be characterized by Dyson equations associated with its Green functions. Here we use a nonequilibrium diagrammatic description, the Keldysh technique [22, 23], and take the initial conditions to be random. Two Green functions, or rather three *real* functions, are needed to describe the system, they are the retarded and the

statistical (or Keldysh) Green functions, that are defined by

$$G^r(t, t') = -i\Theta(t - t')\overline{\langle s_i(t)s_i(t') - s_i(t')s_i(t) \rangle}, \quad (7)$$

and

$$G^s(t, t') = -i\overline{\langle s_i(t)s_i(t') + s_i(t')s_i(t) \rangle}, \quad (8)$$

respectively. For the $p = 2$ spherical model the Green functions are diagonal in the spin index, due to both the disorder averaging, and the infinite-range nature of the interaction. The retarded Green function is proportional to the “response” in the spin glass nomenclature, while the statistical Green function is proportional to the “correlation”. At equal times we demand that $G^s(t, t) = -2i$ due to the spherical constraint, thus setting $z(t)$.

When a system is at equilibrium the Green functions that describe it are a function of the time difference only. In that case one can Fourier transform $G^r(t - t')$ and $G^s(t - t')$ over the time difference to obtain $\tilde{G}^r(\omega)$ and $\tilde{G}^s(\omega)$. Furthermore, at equilibrium the retarded and the statistical Green functions are related via the fluctuation-dissipation theorem (FDT)

$$\tilde{G}^s(\omega) = 2i \coth\left(\frac{\omega}{2T}\right) \text{Im}\tilde{G}^r(\omega), \quad (9)$$

where T is the equilibrium temperature of the system. When the spin system is in the paramagnetic phase, it is in equilibrium, and therefore it obeys FDT. Although in the coarsened phase the system is *not* in equilibrium, we will show that one can identify unique stationary contributions to the retarded and the statistical Green functions, that are related via the FDT, where the temperature is that of the bath.

When the spin system is in the coarsened phase, the Green functions depend on *both* times, and not only on the time difference. The spin Green functions in the time domain obey the Dyson equations

$$-\left[m\frac{\partial^2}{\partial t^2} + z(t)\right]G^r(t, t') = \delta(t - t') + \int dt'' \Sigma^r(t, t'')G^r(t'', t'), \quad (10)$$

and

$$-\left[m\frac{\partial^2}{\partial t^2} + z(t)\right]G^s(t, t') = \int dt'' [\Sigma^s(t, t'')G^a(t'', t') + \Sigma^r(t, t'')G^s(t'', t')], \quad (11)$$

where $G^a(t, t') = [G^r(t', t)]^*$ is the advanced Green function, and $\Sigma^{r/s}(t, t')$ are the self-energy functions. Note that the Dyson equations above apply to the system in the paramagnetic

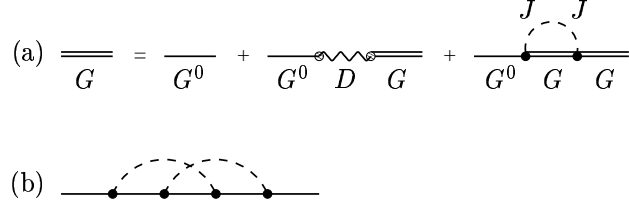


FIG. 1: (a) Dyson equations depicted diagrammatically in a schematic manner, in the self-consistent-Born approximation. The dashed lines represent averaging over spin-spin interaction. (b) An example of a diagram with crossed spin-spin interaction averaging lines, that is proportional to $1/N$, and therefore is neglected in our calculation.

phase also, where $z(t)$ is a constant and all other functions depend only on the time difference. Assuming N is large, we consider the self-energy functions in the self-consistent-Born approximation [see Fig. 1(a)], in which case they are given by

$$\Sigma^{r/s}(t, t') = D^{r/s}(t - t') + J^2 G^{r/s}(t, t'). \quad (12)$$

The bath contributions to the self-energy, which include the spin-bath interaction vertices, are $D^{r/s}(t - t')$. We have neglected “crossing” diagrams [e.g., see Fig. 1(b)], since they are at least a factor of $1/N$ smaller than the diagrams considered. This approximation is exact in the $N \rightarrow \infty$ limit.

We remark that the equation for the retarded Green function (10) is completely decoupled from the statistical Green function. This is a result of two model-dependant features: (i) that $p = 2$, (ii) that the coupling to the bath is linear in the spin operators. In a $p \geq 3$ model, or in any p model with a nonlinear coupling to the bath, the equation for the retarded Green function would include the statistical Green function as well.

The detailed nature of the relaxation of a spin system far from equilibrium depends on the time it has spent in its low-temperature phase before the start of the measurement. This phenomenon is known as aging. This dynamical behavior has been described using scaling and other phenomenological approaches [19, 24]. More recently aging has been studied analytically in microscopic models where mean-field models are exact [19, 24]. It was realized that in these infinite-range systems the time evolution is dominated by motion in flat directions in phase space rather than by transitions over barriers; with random initial conditions, the system continues to evolve and never approaches its local equilibrium. For

this “weak-ergodicity” breaking scenario [19, 24–26], it is crucial that the dimensionality of phase space is very large. Because the spin system is out of equilibrium, its memory of its initial states will depend specifically on the time when the measurement commenced, t' , and the time when it ended, $t = t' + \Delta t$, and not simply the time difference, $\Delta t = t - t'$. In the weak-ergodicity breaking scenario, if the waiting-time t' is finite, the system can evolve in the long-time limit so as to lose complete memory of its initial configuration at t' . This assumption of weak long-term memory has been shown to be self-consistent for several classical long-range glassy and coarsened models [19, 24–26]. In the quantum case, it is expected to hold in general [1, 2], though it may be violated near a quantum critical point where the decoherence time diverges.

We assume that the weak-ergodicity breaking scenario applies to our system, and look for a solution that obeys it. More specifically, according to the weak-ergodicity breaking scenario, one expects the statistical Green function to decay in the following manner

$$\lim_{t' \rightarrow \infty} G^s(t, t') = -2iq + G_{\text{ST}}^s(t - t'), \quad (13)$$

$$\lim_{t-t' \rightarrow \infty} G_{\text{ST}}^s(t - t') = 0, \quad (14)$$

$$\lim_{t \rightarrow \infty} G^s(t, t') = 0, \quad (15)$$

for $t \geq t'$. The Edwards-Anderson parameter, $q = -\lim_{t-t' \rightarrow \infty} \lim_{t' \rightarrow \infty} G^s(t, t')/2i$, characterizes the spin glass, or the coarsened phase. For large waiting times t' , the statistical Green function is given by a term that is proportional to q , plus a stationary function $G_{\text{ST}}^s(t - t')$ that decays to zero at infinity. This serves as a definition of $G_{\text{ST}}^s(t - t')$.

Using the definition for $G_{\text{ST}}^s(t - t')$, the statistical Green function for any times t' and t can be written as a sum of $G_{\text{ST}}^s(t - t')$ and an aging function $G_{\text{AG}}^s(t, t')$, that is not time translationally invariant,

$$G^s(t, t') = G_{\text{AG}}^s(t, t') + G_{\text{ST}}^s(t - t'). \quad (16)$$

At equal times $G^s(t, t) = -2i$ due to the spherical constraint, so that Eq. (13) at equal times yields

$$\lim_{t \rightarrow \infty} G_{\text{AG}}^s(t, t) = -2iq \quad \text{and} \quad G_{\text{ST}}^s(0) = -2i(1 - q). \quad (17)$$

In order to write the Dyson equations (10)-(11), we need the contribution of the bath to the self-energy [see (12)]. In the frequency domain the free-bath Green functions for mode

a , that are associated with the free-bath Hamiltonian \mathcal{H}_B , are given by

$$\tilde{D}_a^r(\omega) = \frac{1}{\omega - \omega_a + i\delta/2} - \frac{1}{\omega + \omega_a + i\delta/2}, \quad (18)$$

$$\tilde{D}_a^s(\omega) = -2\pi i \coth\left(\frac{\omega}{2T}\right) [\delta(\omega - \omega_a) + \delta(\omega + \omega_a)], \quad (19)$$

where T is the bath temperature. Fourier transforming into the time domain one obtains

$$D_a^r(t) = -2\Theta(t) \sin \omega_a t, \quad (20)$$

$$D_a^s(t) = -2i \coth\left(\frac{\omega_a}{2T}\right) \cos \omega_a t. \quad (21)$$

We assume that the bath is in equilibrium, namely that it is so large that it is unaffected by its interaction with the spin system. Therefore we take the bath Green functions to be those in (18) and (19), that depend only on the time difference. Thus the contributions of the bath to the self-energy are also time-translationally invariant. Furthermore, they are linear in the bath Green functions. They are obtained by multiplying the Green function of each mode by its density of states, $(2M_a\omega_a)^{-1}$, and by the spin-bath coupling constant squared C_a^2 , and summing over all modes

$$D^r(t) = -2\Theta(t) \int_{-\infty}^{\infty} d\omega I(\omega) \sin \omega t, \quad (22)$$

for the retarded self-energy, and

$$D^s(t) = -2i \int_{-\infty}^{\infty} d\omega I(\omega) \coth\left(\frac{\omega}{2T}\right) \cos(\omega t), \quad (23)$$

for the statistical self-energy, where [20]

$$I(\omega) = \sum_{a=1}^{N_b} \frac{C_a^2}{2M_a\omega_a} \delta(\omega - \omega_a). \quad (24)$$

The bath temperature T enters the equations for the spin Green functions only through the bath contribution to the statistical self-energy.

In the case of an Ohmic bath $I(\omega) = (\gamma\omega/\pi) \exp(-|\omega|/\Omega)$ [20], where γ is a dimensionless coupling constant, and Ω is an ultraviolet cutoff that will be taken to infinity later on. Thus for the case of an Ohmic bath

$$D^r(t) = \frac{4\gamma}{\pi} \Theta(t) \frac{d}{dt} \frac{\Omega}{1 + (\Omega t)^2}. \quad (25)$$

When $\Omega \rightarrow \infty$ one can Fourier transform (25) and obtain

$$\tilde{D}^r(\omega) = -2\gamma \left(\frac{2\Omega}{\pi} + i\omega \right) \equiv \tilde{D}^r(0) + \tilde{d}^r(\omega). \quad (26)$$

It would seem that since $\tilde{D}^r(0) \propto \Omega$, the limit $\Omega \rightarrow \infty$ is problematic. However, as we will show, $\tilde{D}^r(0)$ disappears from the equations for the spin Green functions. Since the bath is in equilibrium it must obey the fluctuation-dissipation theorem, so that $\tilde{D}^s(\omega) = 2i \coth(\omega/2T) \text{Im}\tilde{D}^r(\omega)$. Thus

$$\tilde{D}^s(\omega) = -4i\gamma\omega \coth\left(\frac{\omega}{2T}\right). \quad (27)$$

This result can also be obtained from (23) with the Ohmic density of states, directly.

IV. STATIONARY REGIME

In this section we treat the retarded Green function $G^r(t, t')$ at large times t and t' , such that $t, t' \rightarrow \infty$, while $t - t'$ is finite. We show that it is stationary, and that it is related to the stationary part of the statistical Green function via the fluctuation-dissipation theorem.

The Lagrange multiplier $z(t)$ is simply a function of one time variable, therefore for large t it should saturate to a constant value $z_\infty = \lim_{t \rightarrow \infty} z(t)$. We assume that in the coarsened phase z_∞ is independent of temperature, which indeed turns out to be consistent with our findings. Since D^r is independent of temperature, from Eq. (10) it is evident that once $z(t)$ saturates to z_∞ , $G^r(t, t')$ no longer depends on temperature. This agrees with the classical result found in [18]. Since $G^r(t, t')$ does not depend on G^s , which is expected to age, one can find a time-translational solution for G^r , once z_∞ is approached. This is a peculiarity of the $p = 2$ model, with the linear spin-bath coupling, since the retarded Green function is independent of the statistical Green function. We note that, consistent with our present discussion, no aging was found in the response of the infinite-range M -component rotors in the limit $M \rightarrow \infty$ [5].

The time-translational invariance of G^r for large times can be understood from a heuristic point of view. The static solution to the $p = 2$ model is a symmetric double-well in the energy landscape [17, 18]. Since the response in this problem, proportional to $G^r(t, t')$, is temperature-independent, it suffices to consider its behavior in the $T \rightarrow 0$ limit. Here this quantum system is expected to reside deep in one or both wells. The system's response

should not depend on the fact that the system is evolving into both valleys, since they are symmetric. By contrast, the statistical Green function, that is proportional to the spin correlation, is temperature-dependent and does depend on whether the system evolves into a specific minimum or into both of them.

Assuming large enough times so that $z(t)$ has saturated, and therefore $G^r(t, t') = G^r(t-t')$, one can Fourier transform Eq. (10) over $t - t'$ to obtain

$$\tilde{G}^r(\omega) = \frac{1}{m\omega^2 - \bar{z} - \tilde{d}^r(\omega) - J^2\tilde{G}^r(\omega)}, \quad (28)$$

where $\bar{z} = z_\infty + \tilde{D}^r(0)$. This is a quadratic equation for $\tilde{G}^r(\omega)$ which also applies to the paramagnetic regime. However, \bar{z} is still unknown, and will be obtained from the equation for the statistical Green function. It will be shown that \bar{z} is finite, so that the divergence of $\tilde{D}^r(0)$ for $\Omega \rightarrow \infty$ does not pose a problem.

In order to obtain an equation for G_{ST}^s , we write the statistical self-energy in terms of the stationary and aging contributions, $\Sigma^s(t, t') = \Sigma_{\text{ST}}^s(t - t') + \Sigma_{\text{AG}}^s(t, t')$, where

$$\Sigma_{\text{ST}}^s(t - t') = D^s(t - t') + J^2 G_{\text{ST}}^s(t - t'), \quad (29)$$

$$\Sigma_{\text{AG}}^s(t, t') = J^2 G_{\text{AG}}^s(t, t'). \quad (30)$$

Assuming t' is large, we substitute (13) into Eq. (11) and obtain

$$\begin{aligned} - \left(m \frac{\partial^2}{\partial t^2} + z_\infty \right) [-2iq + G_{\text{ST}}^s(t - t')] = \\ \int_{-\infty}^{\infty} dt'' [\Sigma_{\text{ST}}^s(t - t'') G^a(t'' - t') + \Sigma^r(t - t'') G_{\text{ST}}^s(t'' - t')] - \\ 2iq [2J^2 \tilde{G}^r(0) + \tilde{D}^r(0)]. \end{aligned} \quad (31)$$

In the derivation of Eq. (31), one encounters terms of the form $\int_{-\infty}^{\infty} dt'' G_{\text{AG}}^s(t, t'') F(t'' - t')$, where F can be any one of the stationary functions $G^{r/a}$ or $D^{r/a}$. We note that in these terms the aging function changes slowly compared to the stationary ones. We exploit this feature and assume that t'' is close to t' , since the retarded and advanced functions decay to zero when their arguments become large. We therefore approximate

$$\int_{-\infty}^{\infty} dt'' G_{\text{AG}}^s(t, t'') F(t'' - t') \simeq -2iq \tilde{F}(0), \quad (32)$$

where $\tilde{F}(\omega)$ is the Fourier transform of $F(t)$. Similarly,

$$\int_{-\infty}^{\infty} dt'' F(t - t'') G_{\text{AG}}^s(t'', t') \simeq -2iq \tilde{F}(0). \quad (33)$$

In addition, in obtaining Eq. (31), we used the fact that the imaginary part of a retarded Green function at zero frequency is zero.

Although we assumed that $t - t'$ is finite, we can Fourier transform Eq. (31) since it applies to *any* $t - t'$ in the $t' \rightarrow \infty$ limit. The Fourier transform of Eq. (31) is

$$\left\{ m\omega^2 - \bar{z} - \tilde{d}^r(\omega) - J^2 \left[\tilde{G}^r(\omega) + \tilde{G}^a(\omega) \right] \right\} \tilde{G}_{ST}^s(\omega) = \tilde{D}^s(\omega) \tilde{G}^a(\omega) - 2iq \delta(\omega) \left[2J^2 \tilde{G}^r(0) + \bar{z} \right]. \quad (34)$$

Since $\lim_{t \rightarrow \infty} G_{ST}^s(t) = 0$ the expression for $\tilde{G}_{ST}^s(\omega)$ cannot include terms that are proportional to $\delta(\omega)$. We expect the other Green functions in Eq. (34) to be similarly well-behaved. Therefore in the coarsened phase, since q is finite, the term in the square brackets that multiplies the delta function must be zero, leading to the following equation for \bar{z} and $\tilde{G}^r(0)$

$$\bar{z} = -2J^2 \tilde{G}^r(0). \quad (35)$$

In the paramagnetic phase $q = 0$, and therefore Eq. (35) is no longer valid.

Another equation for \bar{z} and $\tilde{G}^r(0)$ is found by substituting $\omega = 0$ into Eq. (28),

$$\bar{z} = -\frac{1}{\tilde{G}^r(0)} - J^2 \tilde{G}^r(0), \quad (36)$$

which when compared with Eq. (35) renders $[J\tilde{G}^r(0)]^2 = 1$. Since \tilde{G}^r must be analytic in the upper half plane, one obtains $\tilde{G}^r(0) = -1/J$ and therefore

$$\bar{z} = 2J, \quad (37)$$

in the coarsened phase. Indeed as we anticipated, \bar{z} is a constant and does not depend on the temperature T . Furthermore, \bar{z} is finite, so the divergence of $\lim_{\Omega \rightarrow \infty} \tilde{D}^r(0)$ is not a problem; see the definition of \bar{z} following Eq. (28), and the discussion following (26). The same \bar{z} has been found for the classical $p = 2$ model [17]. In Ref. [2] an expression for z_∞ in the quantum $p \geq 3$ models was found from an equation that was written for the aging part of the response. However, since in the $p = 2$ case the retarded Green function at large times is stationary, that approach to the solution is not applicable here.

Now that \bar{z} is known, we can solve Eq. (28) for $\tilde{G}^r(\omega)$ in the coarsened phase

$$\tilde{G}^r(\omega) = \frac{1}{2J^2} \left\{ m\omega^2 - 2J + 2i\gamma\omega - \left[(m\omega^2 + 2i\gamma\omega) (m\omega^2 - 4J + 2i\gamma\omega) \right]^{1/2} \right\}. \quad (38)$$

In solving the quadratic equation for $\tilde{G}^r(\omega)$, we choose the negative sign in front of the square root to ensure that $\lim_{\omega \rightarrow \infty} \tilde{G}^r(\omega) = 0$.

We now demonstrate the FDT in the coarsened phase for the stationary part of the Green functions. Using Eq. (28) in Eq. (34), after the term with the delta function has been eliminated, we obtain

$$\tilde{G}_{ST}^s(\omega) = \frac{\tilde{D}^s(\omega) |\tilde{G}^r(\omega)|^2}{1 - J^2 |\tilde{G}^r(\omega)|^2}. \quad (39)$$

We write $\tilde{D}^s(\omega)$ in terms of $\text{Im}\tilde{D}^r(\omega)$ via the FDT, and taking the imaginary part of Eq. (28) we obtain

$$\tilde{G}_{ST}^s(\omega) = 2i \coth\left(\frac{\omega}{2T}\right) \text{Im}\tilde{G}^r(\omega). \quad (40)$$

Thus, we have shown that the stationary part of the statistical Green function is related to the imaginary part of the retarded Green function via the fluctuation-dissipation theorem, where the temperature is that of the bath. Usually this relation is taken as an ansatz [1–5]. However, in this specific case of the $p = 2$ model with the linear spin-bath coupling, we have demonstrated it explicitly.

Now we have fully solved for the system's behavior in the stationary regime. Once the retarded Green function has been found, (38), the stationary part of the statistical Green function is known as well via the FDT, (40).

V. THE EDWARDS-ANDERSON ORDER PARAMETER

The Edwards-Anderson order parameter q can be found by substituting the expression that was obtained for the stationary part of the statistical Green function, (40) (FDT), into the matching condition at zero time difference (17):

$$q = 1 + \int_{-\infty}^{\infty} \frac{d\omega}{2\pi} \coth\left(\frac{\omega}{2T}\right) \text{Im}\tilde{G}^r(\omega). \quad (41)$$

The Edwards-Anderson parameter is in the range $0 \leq q \leq 1$. We expect to obtain $q = 0$ at equilibrium for the system in its paramagnetic phase. We note that (41) admits negative values of q , which correspond to an instability of the coarsened phase; in this case one should look for a paramagnetic solution.

As a check, expression (41) for q can be evaluated in two known limits. The first is at high temperatures, when T is much larger than all energy-scales apart from J . In this case

$\coth(\omega/2T) \simeq 2T/\omega$ and we obtain

$$q = 1 + \frac{T}{\pi} \int_{-\infty}^{\infty} \frac{d\omega}{\omega} \text{Im}\tilde{G}^r(\omega) = 1 + T \text{Re}\tilde{G}^r(0) = 1 - \frac{T}{J}, \quad (42)$$

where we have used the Kramers-Kronig relation. This is the well-known classical result [17, 18], which should indeed be obtained when T is large. As an aside, we note that T should be smaller than J , since otherwise the system would undergo a phase transition into the paramagnetic phase.

The other limit that we can check is $T \rightarrow 0$, since $\lim_{T \rightarrow 0} \coth(\omega/2T) = \text{sign}(\omega)$; in this case

$$q = 1 + \int_{-\infty}^{\infty} \frac{d\omega}{2\pi} \text{sign}(\omega) \text{Im}\tilde{G}^r(\omega). \quad (43)$$

If the system is in equilibrium, $\int_{-\infty}^{\infty} d\omega/(2\pi) \text{sign}(\omega) \text{Im}\tilde{G}^r(\omega) = -1$ [27] and we obtain $q = 0$, as expected.

In our calculation of q we will use the following approximation

$$\coth\left(\frac{\omega}{2T}\right) \simeq \begin{cases} \text{sign}(\omega) & \text{for } 2T < \omega, \\ 2T/\omega & \text{for } 2T > \omega, \end{cases} \quad (44)$$

so that

$$q \simeq 1 + \frac{2T}{\pi} \int_0^{2T} \frac{d\omega}{\omega} \text{Im}\tilde{G}^r(\omega) + \frac{1}{\pi} \int_{2T}^{\infty} d\omega \text{Im}\tilde{G}^r(\omega). \quad (45)$$

We are aware that the model we are using for a bath can lead to peculiar results since it does not incorporate an infrared cutoff for the bath frequencies. In such a case the first integral in Eq. (45) might be finite even when $T \rightarrow 0$. We have verified that this problem does not arise in our calculations, since for $\omega \rightarrow 0$ $\text{Im}\tilde{G}^r(\omega) \propto \omega^\alpha$, where $\alpha \geq 1$.

For a given average spin-spin interaction J we look at the phase space that is defined by the parameters m, γ , and T . We focus on the $\gamma \rightarrow 0$, and the $T = 0$ planes. The coarsened phase is defined by a finite q . We shall look for the $q = 0$ line, knowing that beyond it (when $q < 0$) the coarsened phase breaks down, and the system must be in the paramagnetic phase. We have checked numerically in the $\gamma \rightarrow 0$ and the $T = 0$ planes, that there is no coexistence of the paramagnetic and the coarsened phases, except on the $q = 0$ line. Furthermore, in section VIB we show that the paramagnetic solution changes continuously into the coarsened one. Thus this is a second order phase transition, and the $q = 0$ line that is found in the coarsened phase is indeed the phase boundary.

In the next section we describe the phase diagram. Here we concentrate on finding the quantum critical point which resides in the $T = 0$ plane at the $\gamma \rightarrow 0$ limit. We expect the system to behave in a coarsened manner for larger values of m . Upon decreasing m we anticipate that the quantum fluctuations will grow until the mass reaches a critical value m^* , where the system undergoes a phase transition into the paramagnetic state.

At this point we comment on the physical meaning of taking $\gamma \rightarrow 0$. If one were to take $\gamma = 0$ from the start, one would initially decouple the spin system from the bath. In this case the FDT relationship that we had found, (40), that includes the bath temperature, would not be valid—the spin system would not be “aware” of the bath’s temperature unless it was coupled to it at some point in time. By taking $\gamma \rightarrow 0$ we consider the spin system to be coupled to the bath, with an infinitesimally small coupling.

Substituting $\gamma \rightarrow 0$ into Eq. (38), we find

$$\text{Im}\tilde{G}^r(\omega)\Big|_{\gamma\rightarrow 0} = -\frac{1}{J}\left(\frac{m}{J}\right)^{1/2}\omega\left(1 - \frac{m\omega^2}{4J}\right)^{1/2} \quad \text{for } |\omega| < 2\left(\frac{J}{m}\right)^{1/2}, \quad (46)$$

and 0 otherwise. Substituting (46) into Eq. (43) for $T = 0$, one can calculate q exactly

$$q = 1 - \frac{4}{3\pi\sqrt{mJ}}. \quad (47)$$

Taking $q = 0$ in (47) and solving for m we find the quantum critical point

$$m^* = \left(\frac{4}{3\pi}\right)^2 \frac{1}{J} \sim 0.18\frac{1}{J}. \quad (48)$$

We observe that this quantum critical point is identical to that found for the model of $M \rightarrow \infty$ infinite-range quantum rotors [12, 13]. This was originally identified using replica methods which are tricky for quantum phase transitions since the ratio of the replica index to the temperature (M/T) must be kept fixed while $M \rightarrow \infty$ and $T \rightarrow 0$. It was also found using an asymptotic dynamical treatment, and it is reassuring that we recover the same result in the limit of zero dissipation for a treatment of a more general Hamiltonian. As an aside, it is interesting to note that, to date, the only other glassy quantum critical point has been found in the periodic Josephson junction array, also in the limit of zero dissipation [11].

VI. THE PHASE DIAGRAM

Using q and \bar{z} as probes we now characterize the phase space that is spanned by the variables γ, m and T , by identifying the coarsened and the paramagnetic regions. When the system is in the coarsened phase, $\bar{z} = 2J$ [see (37)], and $q \neq 0$ varies. The $q = 0$ line in the γ, m, T phase space tells us when the coarsened phase becomes unstable. In the paramagnetic phase $q = 0$ since the system is in equilibrium, and \bar{z} varies. The spin-spin interaction is important in the coarsened phase, and indeed \bar{z} depends on J . In the paramagnetic phase we expect \bar{z} to depend on the two important energies $1/m$ and T .

The system's phase behavior is presented in two sections, VIA and VIB, associated with the coarsened and the paramagnetic phases respectively. In the coarsened phase $\bar{z} = 2J$, and we characterize the behavior of q . By contrast, the system is in equilibrium in the paramagnetic phase, so that $q = 0$ and we look for \bar{z} . Ultimately we show that \bar{z} changes continuously from the paramagnetic value to the coarsened one. The phase behavior in the $\gamma \rightarrow 0$ plane is displayed in Fig. 2, and in Fig. 3 we present our findings in the $T = 0$ plane. In Fig. 4 we show the transition lines in the $T - m$ plane for several values of γ , determined by a numerical calculation. Since subsections VIA and VIB include our calculations, they are rather technical. For a summary of our results, we refer the reader to Tables I and II, which are depicted graphically in Figs. 2, 3, and 4. The main qualitative features of the system's phase behavior are summarized in section VII.

A. The coarsened phase

In the coarsened phase $\bar{z} = 2J$, and q varies; In Table I we summarize the expressions obtained for q in the $\gamma \rightarrow 0$ and $T = 0$ planes. We identify the $q = 0$ line as a second order phase boundary, where the paramagnetic solution changes continuously into the coarsened one, as it will be shown in section VIB.

1. The $\gamma \rightarrow 0$ plane

Results (A) and (B) in Table I are obtained for $\gamma \rightarrow 0$, by substituting the exact expression (46) for $\text{Im}\tilde{G}^r|_{\gamma=0}$, into Eq. (45), and performing the integration. This part of the phase

TABLE I: The Edwards-Anderson parameter q in the coarsened phase, for different regions of the phase space spanned by m, γ and T ; recall that here $\bar{z} = 2J$. The region labels CC, IC, and QC are according to Fig. 2 and Fig. 3

	m, γ and T	$q(m, \gamma, T)$	
(A)	$\gamma \rightarrow 0$ $T > \sqrt{J/m}$	$1 - \frac{T}{J}$	CC
(B)	$\gamma \rightarrow 0$ $T < \sqrt{J/m}$	$1 - \frac{4}{3\pi\sqrt{mJ}} (1 - x^2)^{1/2} \left(1 + \frac{x^2}{2}\right) - \frac{2T}{\pi J} \sin^{-1} x$ where $x = \sqrt{\frac{mT^2}{J}}$	IC
(C)	$\gamma \rightarrow 0$ $T = 0$	$1 - \frac{4}{3\pi\sqrt{mJ}}$	QC
(D)	$T = 0$ $\gamma^2 \ll mJ$	$1 - \frac{4}{3\pi\sqrt{mJ}} \left[1 - \frac{21}{16} \frac{\gamma}{\sqrt{mJ}} - \frac{3}{32} \frac{\gamma^2}{mJ} \ln \frac{\gamma^2}{mJ} + \mathcal{O}\left(\frac{\gamma}{\sqrt{mJ}}\right)^2\right]$	QC
(E)	$T = 0$ $\gamma^2 \gg mJ$	$1 - \frac{1}{2\pi\gamma} \ln \frac{2\gamma^2}{mJ} - \mathcal{O}\left(\frac{1}{\gamma}\right)$	QC

diagram is depicted in Fig. 2. Expression (A) obtained for $T > \sqrt{J/m}$ is the well-known classical result, (42) [17, 18], which depends only on the temperature T . When $T = 0$ and there are only quantum fluctuations, one obtains expression (C) in Table I for q [see also (47)], which depends only on m . Expression (B) that was obtained for $T < \sqrt{J/m}$ has two competing terms: one that is governed by classical dynamics and resembles the classical expression (B), and another that is dominated by quantum fluctuations and is similar to (C). Therefore we call this regime an intermediate region, in which classical and quantum dynamics compete.

We identify the line $T_c(m)$ that corresponds to $q = 0$ in the $m - T$ plane, as the phase boundary between the coarsened and the paramagnetic phases (c.f. solid line in Fig. 2). For $m > 1/J$ the phase transition line is given by $T_c = J$, independent of m . For $m < 1/J$ it is found by setting (B) equal to 0. The line $T_c(m)$ is continuous approaching the point $(m = 1/J, T = J)$ from both directions. Its derivative dT_c/dm is continuous at this point as well, where it becomes zero. For $m < 1/J$ the transition line terminates at the quantum critical point $(m = m^*, T = 0)$ with an infinite derivative $dT_c/dm \rightarrow \infty$.

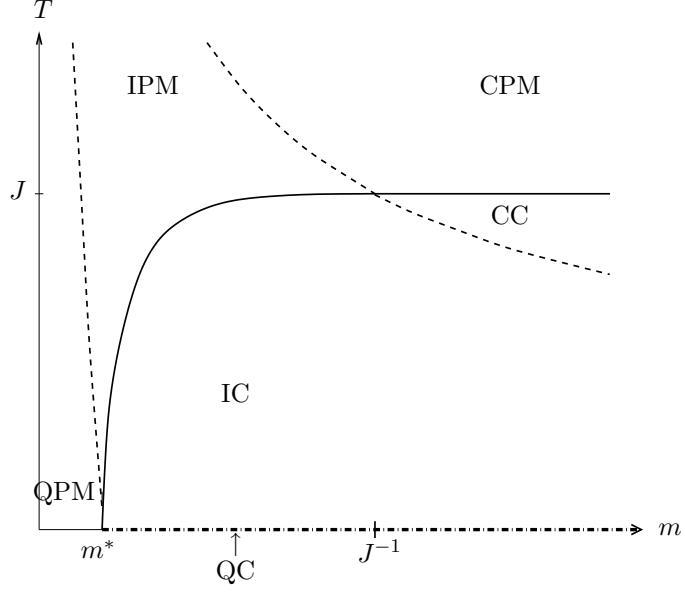


FIG. 2: The phase diagram in the $\gamma \rightarrow 0$ plane. The solid line depicts the second order phase transition line between the paramagnetic and the coarsened phases. One dashed line depicts the border between regions that are dominated by classical dynamics (CPM and CC), and the intermediate ones (IPM and IC) that are governed by both classical and quantum fluctuations. The other dashed line represents the boundary between the intermediate paramagnetic and the quantum paramagnetic (QPM) regimes, where the latter is dominated by quantum dynamics. The quantum coarsened (QC) regime exists only at $T = 0$, for $m > m^*$, the dashed-dotted line.

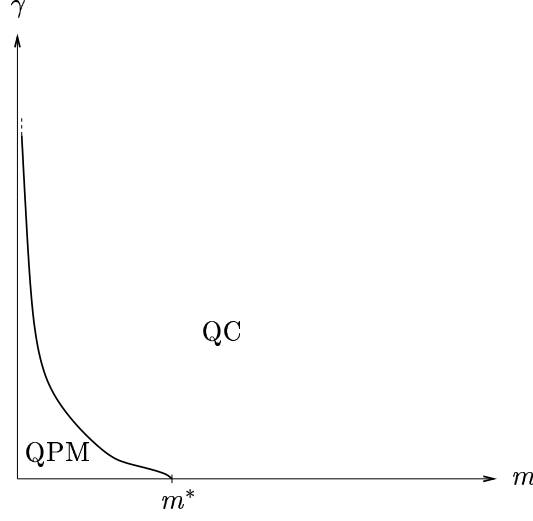


FIG. 3: The phase diagram in the $T = 0$ plane. The solid line depicts the second order phase transition line between the quantum paramagnetic phase (QPM), and the quantum coarsened phase (QC).

2. The $T = 0$ plane

The $T = 0$ plane, depicted in Fig. 3, is by definition entirely quantum. In the weak coupling limit, $\gamma^2 \ll mJ$, we approximate

$$\text{Im}\tilde{G}^r(\omega) \simeq \begin{cases} -\text{Im} \left\{ \frac{1+i}{J} \sqrt{\frac{\gamma\omega}{J} \left(1 - i\frac{m\omega}{2\gamma} \right)} \right\} + \frac{\gamma\omega}{J^2} & \text{for } 0 < \omega < \frac{2\gamma}{m}, \\ -\frac{1}{J} \sqrt{\frac{m\omega^2}{J} \left(1 - \frac{m\omega^2}{4J} \right)} \left[1 + \frac{1}{2} \left(\frac{\gamma}{m\omega} \right)^2 \right] + \frac{\gamma\omega}{J^2} & \text{for } \frac{2\gamma}{m} < \omega < \sqrt{\frac{2J}{m}}, \\ -\frac{1}{J^2} \sqrt{(mJ + \gamma^2)\omega^2 - \frac{(m\omega^2)^2}{4}} + \frac{\gamma\omega}{J^2} & \text{for } \sqrt{\frac{2J}{m}} < \omega < \sqrt{\frac{4J}{m} + \frac{4\gamma^2}{m^2}}, \\ -\frac{2\gamma}{m^2\omega^3} & \text{for } \sqrt{\frac{4J}{m} + \frac{4\gamma^2}{m^2}} < \omega. \end{cases} \quad (49)$$

Substituting these expressions into Eq. (43) we obtain (D) in Table I.

The $m = 0$ case is the extreme limit of strong coupling, $\gamma^2 \gg mJ$. In order to demonstrate that there are no coarsened solutions with $m = 0$, we substitute the imaginary part of the

exact expression for $\tilde{G}^r(\omega)$, (38), with $m = 0$ into Eq. (43). We find that

$$q = -\lim_{\omega \rightarrow \infty} \frac{1}{2\pi\gamma} \ln \frac{\gamma\omega}{J} \rightarrow -\infty, \quad (50)$$

verifying that the system must be in the paramagnetic phase when $m = 0$.

In the calculation of q for $\gamma^2 \gg mJ$ and $m \neq 0$ we approximate

$$\text{Im}\tilde{G}^r(\omega) \simeq \begin{cases} -\frac{1}{2J^2} \text{Im} \left\{ \sqrt{2i\gamma\omega(2i\gamma\omega - 4J)} \right\} & \text{for } 0 < \omega < J/\gamma, \\ -\frac{1}{2\gamma\omega} & \text{for } J/\gamma < \omega < 2B/m, \\ -\frac{2\gamma}{m^2\omega^3} & \text{for } 2\gamma/m < \omega, \end{cases} \quad (51)$$

from which we find (E) in Table I. The dominant logarithmic part agrees with (50). In order to find the phase boundary for $\gamma^2 \gg mJ$ (c.f. solid line in Fig. 3) we set $q = 0$ in (E) and obtain

$$m = \frac{2\gamma^2}{J} e^{-2\pi\gamma}. \quad (52)$$

Thus the phase boundary for large γ corresponds to an exponentially small m .

From Fig. 3 it is clear that as the coupling to the bath γ is increased, m must decrease in order to cross the transition line. The spin-bath coupling causes a decay of the quantum fluctuations, which in the absence of temperature, are necessary for the system to make the transition from the coarsened to the paramagnetic phases.

3. Finite T and γ

In Fig. 4 we display the phase boundaries $T_c(m)$ for a set of spin-bath couplings γ . We determined these lines numerically, by solving $q|_\gamma(m) = 0$ for T , at a set of m values, where q and \tilde{G}^r are given by (41) and (38) respectively. For constant m at low temperatures, as γ is increased, T must be raised in order to destabilize the coarsened phase. As previously discussed the coupling to the bath causes a decay in the quantum fluctuations. Therefore its effect can be overcome either by decreasing m , thereby increasing the quantum fluctuations, or by increasing T . As an aside we note that at high temperatures, increasing γ has a much smaller effect. Our finding that the position of the transition line depends on the strength of the spin-bath coupling is qualitatively similar to that obtained in recent numerical studies of dissipative effects on more complex quantum systems [28].

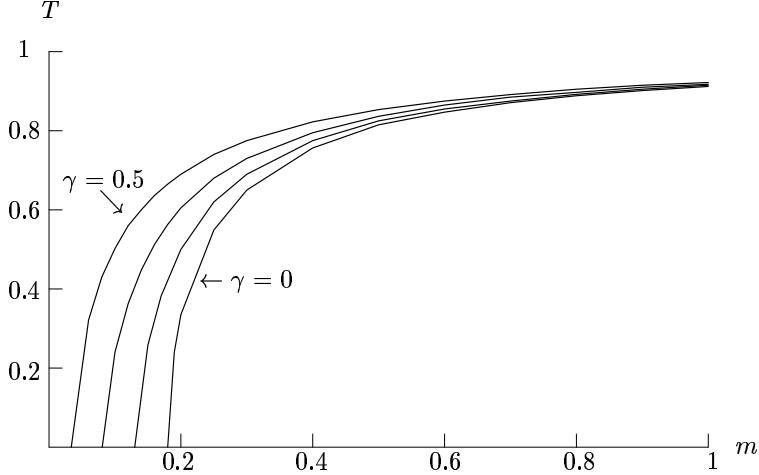


FIG. 4: The $q = 0$ lines in the T versus m plane for $\gamma = 0, 0.1, 0.25$ and 0.5 .

TABLE II: The Lagrange multiplier \bar{z} for different regions of the phase space spanned by m, γ and T , in the paramagnetic phase. The region labels CPM and QPM are according to Figs. 2 and 3

	m, γ and T	$\bar{z}(m, \gamma, T)$	
(F)	$\gamma \rightarrow 0$ $T > \sqrt{\frac{\bar{z} + 2J}{4m}}$	$T \left[1 + \left(\frac{J}{T} \right)^2 \right]$	CPM
(G)	$\gamma \rightarrow 0$ $T < \sqrt{\frac{\bar{z} - 2J}{4m}}$	$\frac{1}{4m} \left[1 + 12(mJ)^2 + \mathcal{O}(mJ)^4 \right]$	QPM
(H)	$T = 0$ $\gamma^2 \ll mJ$	$\frac{1}{4m} \left[1 - \frac{8\gamma}{\pi} + 12(mJ)^2 + \dots \right]$	QPM
(I)	$T = 0$ $\gamma^2 \gg mJ$	$\frac{4\gamma^2}{m} \exp(-2\pi\gamma)$	QPM

B. The paramagnetic phase

The expression for \bar{z} that we found earlier, (37), applies only to the coarsened phase. In order to characterize the paramagnet, we must find an expression for \bar{z} in this regime. Therefore we consider Eq. (45) with \tilde{G}^r given by the result of Eq. (28), substitute $q = 0$, and solve for \bar{z} . In Table II we summarize the results of this calculation.

We remind the reader that Eq. (28) for \tilde{G}^r applies to both the paramagnetic and the

coarsened phases, where their difference lies in their respective values of \bar{z} . At the transition line, $\bar{z} = 2J$ for both phases. We find that in the paramagnet \bar{z} is larger than its coarsened value of $2J$, and that it decreases continuously to its coarsened value at the transition line. For the cases of $\gamma \rightarrow 0$, and of $T = 0$, we have checked numerically that an attempt to solve $q = 0$ using (28) for \tilde{G}^r , could be obtained beyond the transition line (in the coarsened region) only if \bar{z} continued to decrease below the value of $2J$. Such a solution would incorporate a finite $\text{Im}\tilde{G}^r(\omega)$ at $\omega = 0$ which is unphysical. Thus we deduce that the coarsened and the paramagnetic phases coexist only at a single line, corresponding to a second order phase transition.

Let us begin by finding \bar{z} for large T . From Eq. (28) we know that $\tilde{G}^r(0) = -[\bar{z} + \sqrt{(\bar{z}^2 - 4J^2)}]/2J^2$. For T much larger than all other energy-scales, including J , and for $q = 0$, we find that $q = 0 = 1 + T \text{Re}\tilde{G}^r(0)$ [following Eq. (42)], and therefore

$$\bar{z} = T \left(1 + \frac{J^2}{T^2} \right), \quad (53)$$

in agreement with the classical result [17]. Note that when $T = J$ and the $q = 0$ line is approached, we obtain $\bar{z} = 2J$ from (53); e.g., for the specific case of $\gamma \rightarrow 0$, see the solid line for $m > 1/J$ in Fig. 2. Thus \bar{z} , and therefore also $\tilde{G}^r(\omega)$ and $\tilde{G}^s(\omega)$ change continuously when $q = 0$, and indeed $T = J$ is a second order phase transition line.

1. The $\gamma \rightarrow 0$ plane

Substituting $\gamma \rightarrow 0$ in Eq. (28) and solving for \tilde{G}^r , we find that

$$\text{Im}\tilde{G}^r(\omega) = -\frac{1}{J} \sqrt{1 - \left(\frac{m\omega^2 - \bar{z}}{2J} \right)^2} \quad \text{for } \omega_- < \omega < \omega_+, \quad (54)$$

where $\omega_{\pm} = \sqrt{(\bar{z} \pm 2J)/m}$, and $\text{Im}\tilde{G}^r = 0$ otherwise.

If $2T > \omega_+$, we use (45) to calculate q , and then, substituting $q = 0$ we obtain the following equation for \bar{z} ,

$$\frac{2T}{\pi J} \int_{\omega_-}^{\omega_+} \frac{d\omega}{\omega} \sqrt{1 - \left(\frac{m\omega^2 - \bar{z}}{2J} \right)^2} = 1. \quad (55)$$

The exact result of the integration on the left hand side is a combination of elliptic functions, from which it is hard to isolate \bar{z} . We will therefore expand in $2J/\bar{z}$. It is convenient to

make a change of variables $\sin \theta = (m\omega^2 - \bar{z})/2J$. This procedure leads to expression (F) in Table II for \bar{z} [see also (53)]. Substituting this expression for \bar{z} into ω_+ we find the line $T = \omega_+/2$, the boundary between the IPM and the CPM regions above which the system seems to be predominantly classical (c.f. dashed line in Fig. 2).

For $2T < \omega_-$, we obtain in the same manner as above

$$\frac{1}{\pi} \int_{\omega_-}^{\omega_+} \frac{d\omega}{J} \sqrt{1 - \left(\frac{m\omega^2 - \bar{z}}{2J} \right)^2} = 1. \quad (56)$$

If one neglects $2J/\bar{z}$ completely, the result is

$$\bar{z} = \frac{1}{4m}, \quad (57)$$

in agreement with [8]. This result is valid for $m \ll 1/8J$. In this case $2J/\bar{z} \ll 1$ and our approximation is consistent.

If we continue the expansion up to linear order in $2J/\bar{z}$ we obtain expression (G) in Table II. Substituting m^* into (G) we find $\bar{z} = 1.93J$ which is very close to the expected value of $\bar{z} = 2J$ in the coarsened phase. Thus, it would seem that even close to the transition between the coarsened and the paramagnetic states this is a good approximation. Substituting (G) into the expression for ω_- we were able to draw the line $T = \omega_-/2$, the dashed line between the QPM and the IPM regions in Fig. 2, below which the Lagrange multiplier \bar{z} is governed by quantum behavior.

When $\omega_- < 2T < \omega_+$ the system is in an intermediate regime that is governed by both classical and quantum dynamics (IPM regime in Fig. 2). We define θ_T such that $\sin \theta_T = (4mT^2 - \bar{z})/2J$. Using Eq. (45) in order to calculate q and then setting $q = 0$ we obtain

$$\frac{2T}{\pi} \int_{-\pi/2}^{\theta_T} d\theta \frac{\cos^2 \theta}{\bar{z} + 2J \sin \theta} + \frac{1}{\pi\sqrt{m}} \int_{\theta_T}^{\pi/2} d\theta \frac{\cos^2 \theta}{\sqrt{\bar{z} + 2J \sin \theta}} = 1. \quad (58)$$

Upon expansion in $2J/\bar{z}$ the equation for \bar{z} becomes

$$\begin{aligned} & \frac{2T}{\bar{z}} \left\{ \left(\frac{\theta_T + \pi/2}{2\pi} \right) \left[1 + \left(\frac{J}{\bar{z}} \right)^2 \right] + \frac{2J}{3\pi\bar{z}} \cos^3 \theta_T \right\} + \\ & \frac{1}{\sqrt{m\bar{z}}} \left\{ \left(\frac{\pi/2 - \theta_T}{2\pi} \right) \left[1 + \frac{3}{8} \left(\frac{J}{\bar{z}} \right)^2 \right] - \frac{J}{3\pi\bar{z}} \cos^3 \theta_T \right\} = 1. \end{aligned} \quad (59)$$

Clearly the first term in Eq. (59) describes the classical fluctuations due to temperature, while the second describes the quantum fluctuations due to the mass.

This point can be further clarified by rewriting Eq. (59) in the following form

$$\frac{2T}{\bar{z}} f_1\left(\frac{mT^2}{J}, \frac{\bar{z}}{J}\right) + \frac{1}{\sqrt{m\bar{z}}} f_2\left(\frac{mT^2}{J}, \frac{\bar{z}}{J}\right) = 1, \quad (60)$$

where f_1, f_2 are slowly changing functions of their variables. Neglecting terms of the order of $(J/\bar{z})^2$, for $T = \omega_+/2$, we obtain $f_1 \simeq 1/2$ and $f_2 = 0$, while for $T = \omega_-/2$ we get $f_1 = 0$ and $f_2 \simeq 1/2$. Solving Eq. (60) for \bar{z} as if f_1 and f_2 are known we find that

$$\bar{z} = \frac{f_2^2}{2m} + 2f_1T + \frac{f_2}{2\sqrt{m}} \sqrt{\frac{f_2^2}{m} + 8f_1T}. \quad (61)$$

When $T = \omega_+/2$, Eq. (61) leads to $\bar{z} = T$, while for $T = \omega_-/2$ one obtains $\bar{z} = 1/4m$; the results for $T > \omega_+/2$ and $T < \omega_-/2$ up to the leading order, respectively [c.f. (F) and (G)].

2. The $T = 0$ plane

For $T = 0$ it is convenient to begin our study in the paramagnetic region, far away from the phase boundary. Since the spin-spin interaction is not necessary for the system to be in its paramagnetic state, we can assume at first that $J^2 \ll \min\{4\gamma^2\bar{z}/m, \bar{z}^2\}$, and neglect J in Eq. (28). In this case the retarded Green function is given by $\tilde{G}^{r(0)}(\omega) = (m\omega^2 + 2i\gamma\omega - \bar{z})^{-1}$, where the superscript 0 stands for zeroth order in J . Thus we obtain from Eq. (43) at $q = 0, T = 0$ and $J = 0$ the following equation for \bar{z}

$$\frac{1}{2\pi i \sqrt{m\bar{z} - \gamma^2}} \ln \frac{i\gamma - \sqrt{m\bar{z} - \gamma^2}}{i\gamma + \sqrt{m\bar{z} - \gamma^2}} = 1. \quad (62)$$

In the weak coupling limit, expanding Eq. (62) for $\gamma^2 \ll m\bar{z}$, we find

$$\bar{z} = \frac{1}{4m} \left(1 - \frac{8\gamma}{\pi}\right), \quad (63)$$

which for $\gamma \rightarrow 0$ is consistent with Eq. (57).

Now we reintroduce J iteratively, by considering $\tilde{G}^{r(1)} = (m\omega^2 + 2i\gamma\omega - \bar{z} - J^2\tilde{G}^{r(0)})^{-1}$. We obtain from Eq. (43) at $q = 0$ and $T = 0$ the following equation for \bar{z}

$$\frac{1}{4} \left[\frac{1 - \frac{2}{\pi} \arctan \frac{\gamma}{\sqrt{m(\bar{z}+J) - \gamma^2}}}{\sqrt{m(\bar{z}+J) - \gamma^2}} + \frac{1 - \frac{2}{\pi} \arctan \frac{\gamma}{\sqrt{m(\bar{z}-J) - \gamma^2}}}{\sqrt{m(\bar{z}-J) - \gamma^2}} \right] = 1. \quad (64)$$

Expanding Eq. (64) in $\gamma^2/m\bar{z}$ and in J/\bar{z} , since we expect J to introduce a small correction to \bar{z} in (63), we find (H) in Table II, in agreement with (G) for $\gamma \rightarrow 0$.

Returning to Eq. (62) and assuming strong coupling so that $\gamma^2 \gg m\bar{z}$ we obtain (I), which will equal $2J$ when $m = 2\gamma^2/J \exp(-2\pi\gamma)$. This is exactly the same expression for the transition line that we obtained for the coarsened phase [see (52)]. Thus for large γ the transition is also continuous.

VII. DISCUSSION

In this paper we present a study of the phase behavior of the disordered quantum $p = 2$ spherical model as a function of temperature, dissipation (spin-bath coupling) and strength of quantum fluctuations (mass) at long times, identifying different paramagnetic and coarsened phase regions. Using the weak-ergodicity breaking ansatz and a linear spin-bath coupling, we characterize the system's behavior in the stationary regime. We do so by exploiting the fact that its retarded Green function is independent of its statistical counterpart, and is time-translationally invariant at long-time scales. In doing so, we demonstrate analytically that in the stationary regime the statistical and the retarded Green functions are linked by the fluctuation-dissipation theorem (FDT), a relation usually assumed in studies of quantum glasses with more nonlinearity (e.g. $p \geq 3$ for quantum p spherical models) [1–4].

We use the spherical constraint and the fluctuation-dissipation theorem in the stationary regime to characterize the phase behavior of the system. More specifically, the long-time behavior of \bar{z} , the Lagrange multiplier that enforces the spherical constraint, is crucial for distinguishing different paramagnetic regimes. Similarly the Edwards-Anderson order parameter, q , determined from the stationary statistical Green function (FDT) and matching conditions at equal-times (spherical constraint), characterizes different coarsened phases. We find that all the boundaries between the paramagnetic and the coarsened regions, determined by the $q = 0$ lines, in the $\gamma \rightarrow 0$ and the $T = 0$ planes are continuous; this is in marked contrast to the situation for quantum $p \geq 3$ spherical models where quantum fluctuations at $T = 0$ drive the transition first-order [7–9]. Furthermore, we identify a quantum critical point for $T = 0$ and $\gamma \rightarrow 0$ that coincides with the one found for a model of infinite-range, infinite-component quantum rotors in the absence of dissipation [12, 13].

The Edwards-Anderson order parameter is used to probe the different types of coarsened phases; here \bar{z} is a constant ($\bar{z} = 2J$). More specifically, the behavior of q determines whether the system's dynamics are dominated by classical or by quantum energy-scales. From our

results, it is clear that the increase of either quantum or thermal fluctuations (c.f. Figs. 2 and 3), by raising the inverse-mass or the temperature respectively, leads to the destabilization of the coarsened phase. Furthermore an increase of the spin-bath coupling, γ , causes a decay of the quantum fluctuations; the inverse-mass must be enhanced still further to approach the phase boundary. Finally for constant mass and increasing γ at low temperatures, an increase in T is necessary to cross the $q = 0$ phase boundary (c.f. Fig. 4); the effect of the spin-bath coupling is significantly reduced at higher T .

In the paramagnetic phase, $q = 0$, and the system is characterized by its long-time Lagrange multiplier, \bar{z} , which enforces the spherical constraint. In both the $\gamma \rightarrow 0$ and the $T = 0$ planes (c.f. Figs. 2 and 3, respectively) a quantum paramagnetic phase exists in the limit of vanishing mass. However in the $\gamma \rightarrow 0$ case there are crossovers between different paramagnetic regions as both temperature and mass are increased, corresponding to states where classical energy-scales assume increasing importance compared to their quantum counterparts.

The simplicity of this quantum $p = 2$ spherical model is both its blessing and its curse. It is exactly this feature that permits us to show explicitly the validity of the fluctuation-dissipation theorem in the stationary regime; furthermore this system is accessible to analytic study in the limit of vanishing dissipation. However, we should also point out that here the response is *always* independent of temperature, a feature that makes it particularly awkward for comparison with experiment in the classical and quantum regimes. Furthermore we do not have any spatial information, so possible overlap with real coarsening measurements is rather difficult. However some dialogue between theory and experiment may be possible near the quantum critical point, where issues of length-scales assume reduced importance. As a first step towards making such contact with experiment, we need to establish whether the quantum critical point studied here is in the same universality class as that of the Ising model in a transverse magnetic field. It is intuitive to relate the latter to the $M = 1$ quantum rotor case [12, 30, 31], which would suggest that it is in a different universality class from the $p = 2$ quantum spherical model (that strongly resembles the $M \rightarrow \infty$ case) studied here. However the distinction between continuous and discrete spin symmetries may be important [30], so this argument is inconclusive. On another note, it is known that one can glean spatial information from the study of the classical $p = 2$ spherical model by exploiting a mapping on long time-scales to the three dimensional $O(n)$ model [18, 29], and an analogous mapping

should be explored for the quantum system. Finally we plan to characterize the dynamics of this simple system near its quantum critical point in order to study whether it has any slow relaxational modes that are not shared by its classical counterpart.

Acknowledgments

We would like to thank G. Aeppli, G. Biroli, J. Brooke, L. B. Ioffe, I. Lerner, O. Parcollet, and T. F. Rosenbaum for a number of insightful discussions. This work was partially done at NEC Research Institute. We also acknowledge support from NSF grant 4-21262.

-
- [1] L. F. Cugliandolo and G. Lozano, Phys. Rev. Lett **80**, 4979 (1998).
 - [2] L. F. Cugliandolo and G. Lozano, Phys. Rev. B **59**, 915 (1999).
 - [3] G. Biroli and O. Parcollet, Phys. Rev. B **65**, 094414 (2002).
 - [4] M. P. Kennett and C. Chamon, Phys. Rev. Lett. **86**, 1622 (2001);
 - [5] M. P. Kennett, C. Chamon, and J. Ye, Phys. Rev. B **64**, 224408 (2001).
 - [6] T. Nieuwenhuizen and F. Ritort, Physica A **250**, 8 (1998).
 - [7] L. F. Cugliandolo, D. R. Grempel and C. A. da Silva Santos, Phys. Rev. Lett. **85**, 2589 (2000).
 - [8] L. F. Cugliandolo, D. R. Grempel and C. A. da Silva Santos, Phys. Rev. B **64**, 014403 (2001).
 - [9] G. Biroli and L. F. Cugliandolo, Phys. Rev. B **64**, 014206 (2001).
 - [10] H. Westfahl Jr., J. Schmalian, and P. G. Wolynes, cond-mat/0202099.
 - [11] D. M. Kagan, M. V. Feigel'man, and L. B. Ioffe, Zh. Eksp. Teor. Fiz. **116**, 1450 (1999) [Sov. Phys. JETP **89**, 781 (1999)].
 - [12] J. Ye, S. Sachdev, and N. Read, Phys. Rev. Lett. **70**, 4011 (1993).
 - [13] T. K. Kopec, Phys. Rev. B **50**, 9963 (1994).
 - [14] G. Aeppli and T. F. Rosenbaum, in *Dynamical Properties of Unconventional Magnetic Systems*, edited by A. T. Skjeltorp and D. Sherrington (Kluwer, Netherlands, 1998).
 - [15] J. Brooke, D. Bitko, T. F. Rosenbaum and G. Aeppli, Science **284**, 779 (1999).
 - [16] J. Brooke, T. F. Rosenbaum and G. Aeppli, Nature **413**, 610 (2001).
 - [17] J. M. Kosterlitz, D. J. Thouless and R. C. Jones, Phys. Rev. Lett. **36**, 1217 (1976).
 - [18] L. F. Cugliandolo and D. S. Dean, J. Phys. A **28**, 4213 (1995).

- [19] L. F. Cugliandolo, cond-mat/0210312.
- [20] A. J. Leggett, S. Chakravarty, A. T. Dorsey, M. P. A. Fisher, A. Garg and W. Zwerger, *Rev. Mod. Phys.* **59**, 1 (1987).
- [21] I. V. Lerner, private communication.
- [22] L. V. Keldysh, *Zh. Éksp. Teor. Fiz.* **47**, 1515 (1964) [*Sov. Phys.-JETP* **20**, 1018 (1965)].
- [23] E. M. Lifshitz and L. P. Pitaevskii, *Physical Kinetics*, Vol. 10 of *Course of Theoretical Physics* (Pergamon Press, Oxford, 1981).
- [24] J.-P. Bouchaud, L. F. Cugliandolo, J. Kurchan and M. Mezard in *Spin Glasses and Random Fields*, edited by A. P. Young (World Scientific, Singapore, 1997).
- [25] J.-P. Bouchaud, *J. Phys. I* **2**, 1705 (1992); J.-P. Bouchaud and D. S. Dean, *J. Phys. I* **5**, 265 (1995); C. Monthus and J.-P. Bouchaud, *J. Phys. A* **29**, 3847 (1996); B. Rinn, P. Maass and J.-P. Bouchaud, *Phys. Rev. Lett.* **84**, 5403 (2000).
- [26] L. F. Cugliandolo and J. Kurchan, *Phys. Rev. Lett.* **71**, 173 (1993); *Philos. Mag. B* **71**, 501 (1995).
- [27] G. D. Mahan, *Many-Particle Physics*, (Plenum Press, New York, 1990).
- [28] L. F. Cugliandolo, D. R. Grempel, G. Lozano, H. Lozza, and C. A. da Silva Santos, *Phys. Rev. B* **66**, 014444 (2002).
- [29] A. Barrat, R. Burioni and M. Mezard, *J. Phys. A* **29**, 1311 (1996).
- [30] T. K. Kopec, and R. Pirc, *Phys. Rev. B* **55**, 5623 (1997).
- [31] N. Read, S. Sachdev and J. Ye, *Phys. Rev. B* **52**, 384 (1998).